Bulletin of the New Zealand Society for Earthquake Engineering, Vol. 53, No. 4, December 2020

AUTOMATED STRUCTURAL DYNAMIC MODELLING USING MODEL-FREE HEALTH MONITORING RESULTS

Jeanne Tondut[1], J. Geoffrey Chase[2] and Cong Zhou[3]

(Submitted *August 2019*; Reviewed *October 2019*; Accepted *May 2020*)

ABSTRACT

Structural health monitoring (SHM) methods provide damage metrics and localisation, but not a means of answering subsequent questions concerning immediate or long-term damage mitigation, risk, or safety in re-occupancy. Models based on the SHM results would provide a means to test these issues, but typically require extensive human input, which is not available immediately after an event to enhance and optimise immediate decision-making. This work presents a simple, readily automated modelling approach to translate SHM results from the proven hysteresis loop analysis (HLA) method into foundation models for immediate use. Experimental data from a 3-storey structure tested at the E-Defense facility in Japan are used to assess model performance. The model's ability to capture the essential dynamics is assessed by comparing peak dynamic displacement and cross correlation coefficient (R_{coeff}). For all 6 events, 3 storeys, and 2 directions, median (5-95% Range) of peak displacement error was 0.82 (0.17, 4.09) mm, and average R_{coeff} = 0.82, all of which were significantly improved if the worst event was excluded. Overall, accurate nonlinear, time-varying baseline models were created using data from SHM damage identification and localisation methods using relatively quite simple model structures. The method is readily automated via algorithm, and the models were suitable for initial investigation and analysis on safety, damage mitigation, and thus re-occupancy. Such models could take SHM from being a tool for damage identification and extend it into further decision-making, creating far greater utility for engineers and owners, which could further spur impetus for investment in monitoring.

INTRODUCTION

Increasing urbanisation has magnified seismic risk in seismic zones [1], and the resulting structural damage poses a major risk with significant social and economic impacts. Structural health monitoring (SHM) provides methods to detect, localise, and quantify damage after major events. However, it does no more than deliver this result to experts who assess risk of further damage or collapse in subsequent shocks, as well as any need for immediate or longer-term reinforcement or repair. SHM thus addresses the most immediate needs of responders and leadership.

However, SHM does not provide a ready, quantified tool for assessing these issues or alternatives. A computational model made from the SHM results, and existing building data or/and reasonable surrogates, would enable further analyses to significantly enhance decision-making. However, model creation can be complex, time consuming, and require significant human input. Hence, an automated or semi-automated means of turning SHM results into actionable, reasonably accurate computational models would provide potentially significant benefit. More critically, automated model creation would enable dynamic assessment, potentially also automated, within minutes or hours, providing better data to optimise decision and reduce uncertainty.

There is a wide range of SHM methods available in the literature. Many model-based methods, such as adaptive least mean squares (LMS) and recursive LMS method [2-5], extended Kalman filters (EKF) [6-9] and unscented Kalman filters (UKF) [10-13], identify changes in structural stiffness of selected baseline model parameters to reflect the severity of seismic damage. They are also used to identify Eigen-parameters, such as dynamic frequencies and mode shapes, and their change over an event. However, there is a significant, but unknown, risk of a poor identification result when the chosen model used for SHM does not match the dynamics of the actual measured system response since the actual outcome is not fully known [14, 15].

Other model-based methods, such as the Eigensystem Realization Algorithm [16-20], Flexibility-based methods [21, 22], and finite element model updating method [23, 24] identify stiffness or Eigen-parameters. These approaches also suffer from model-based mismatch errors. They also require the entire measured response to process and are performed off-line after an event, potentially with significant delay if they require human input.

Non-parametric SHM methods relate structural inputs and outputs by a set of equations that may not have explicit physical meaning [25]. Artificial neural networks (ANN) are one of the most common in system identification [26-28] and damage detection [29-32]. However, they can have poor performance due to training or inability to generalise [33]. Others include wavelet analysis [34, 35], genetic algorithms [36, 37] and wireless sensor networks [38, 39]. However, non-parametric SHM methods cannot locate damage without significant a priori knowledge of the structure, creating issues in interpreting or further using the results. Their main advantage is that they are free or relatively independent of assumed models and thus suffer less from errors due to poor model selection.

What is needed for automated structural model generation is a method to accurately identify nonlinear changes in structural stiffness, which is directly correlated to damage. It must do so in real-time or near real-time so results are immediately available. These changes must be available across individual or a few stories to offer enough damage localization to create a

[1] *Master Student, École Nationale d'Ingénieurs de Saint-Étienne, Saint-Étienne, France, jeanne.tondut@enise.fr*
[2] *Distinguished Professor, University of Canterbury, Christchurch, geoff.chase@canterbury.ac.nz*
[3] *Corresponding Author, Post-Doctoral Fellow, University of Canterbury, Christchurch, cong.zhou@canterbury.ac.nz*

useful computational model for evaluating damage severity, solutions, and mitigation. One method shown to meet these criteria is the model-free, mechanics-based hysteresis loop analysis (HLA) method [40-43]. However, as a model-free method, of which there are several, it does not directly yield a model to simulate further outcomes.

This study recreates the HLA identified changes in stiffness for a 3-storey apartment building subjected to 6 ground motion events on the E-Defense shake table in Japan [44]. These identified stiffness trajectories are themselves modelled, and used to create a simplified model of the structure, which could thus be automatically created after an event. To validate this model, simulated ground motions are compared to the measured results, where a good match would indicate.

- The simplified model is able to capture the structural response well at any point in time during the event, and is thus a suitable foundation for further analysis of damage and its immediate or long term mitigation.
- The stiffness values found using HLA for a nonlinear structural response are accurate assessments of the building.

These outcomes would provide a new tool and approach to use SHM results to create models to guide decision making, as well as providing a further more quantified validation of the validity of HLA results not previously presented.

Regarding novelty, this works utilizes existing HLA based SHM results with a proposed, relatively simple model creation method, which together enable easy and simple, and immediate, assessment of amelioration or potential temporary/permanent fixes to stiffness reductions. This outcome is a novel, practical result, as other SHM research stops at damage identification and localization as the end-point. For model-based SHM, the model already exists, but may, as noted, suffer inaccuracies in further analysis if the model does not accurately capture the structure's actual response. Thus, this work thus takes the use of proven, model-free SHM results further to dynamic modelling to aid decision making.

METHODS

Test Structure and E-Defense Shake Table Tests

A full-scale steel moment resisting frame (SMRF) test structure in Figure 1. The right building has added oil dampers in the first storey, and the left is analysed in this work. The three storey's have a uniform height of 2870mm. Seismic weights are 171.85kN, 171.85kN and 90kN for the first, second and third story, respectively. Further structural details are in [44]. Six earthquake excitations were sequentially applied in all three (x,y,z) directions with different magnitudes, as listed in Table 1, at the E-Defense facility in Japan.

Hysteresis Loop Analysis (HLA) and Overall Hypothesis

Hysteresis Loop Analysis (HLA) [40-43] is used to identify building parameters including elastic and plastic stiffness, and yielding displacement. The method extracts significant half cycles of seismic response using sensor data, and extracts linear elastic and nonlinear plastic stiffness values from the hysteretic force-displacement response. Yielding displacement is the maximum deflection prior to plastic deformation, and is thus not based on assumed structural parameter values or mechanics in a baseline model. This mechanics relevant, but model-free approach reduces uncertainty and error [15].

Table 1: Sequential shake table tests and PGA in each direction (x,y,z).

Test No	Input event	PGA(g)		
		y-direction	x-direction	Vertical z-direction
#01	BSL2-18%	0.11	0.13	0.01
#02	Sannomal	0.22	0.16	0.01
#03	Uemachi	0.30	0.35	0.01
#04	Toshin-Seibu	0.62	0.63	0.06
#05	Sannomal	0.21	0.15	0.01
#06	Nankai-Trough	0.87	0.74	0.03

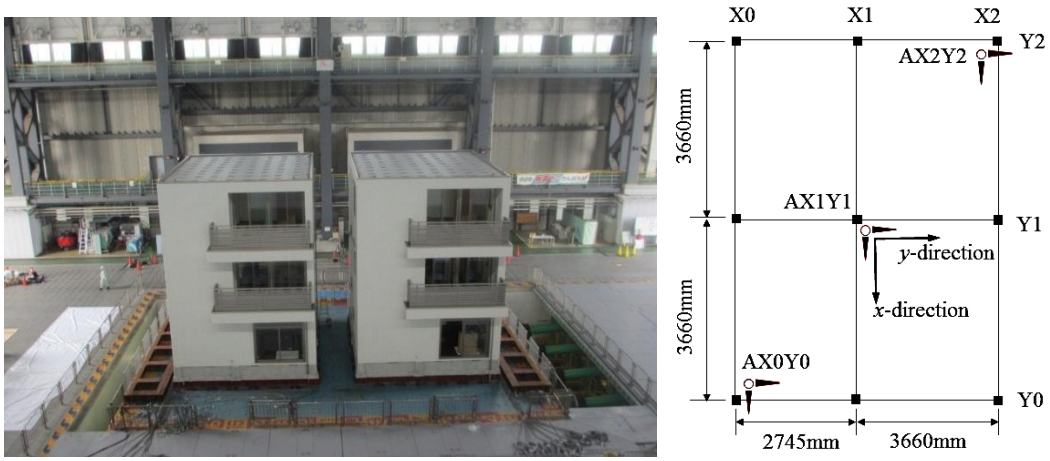

Figure 1: Photo of E-Defense test structure (left) and plan dimensions showing accelerometer placement (right).

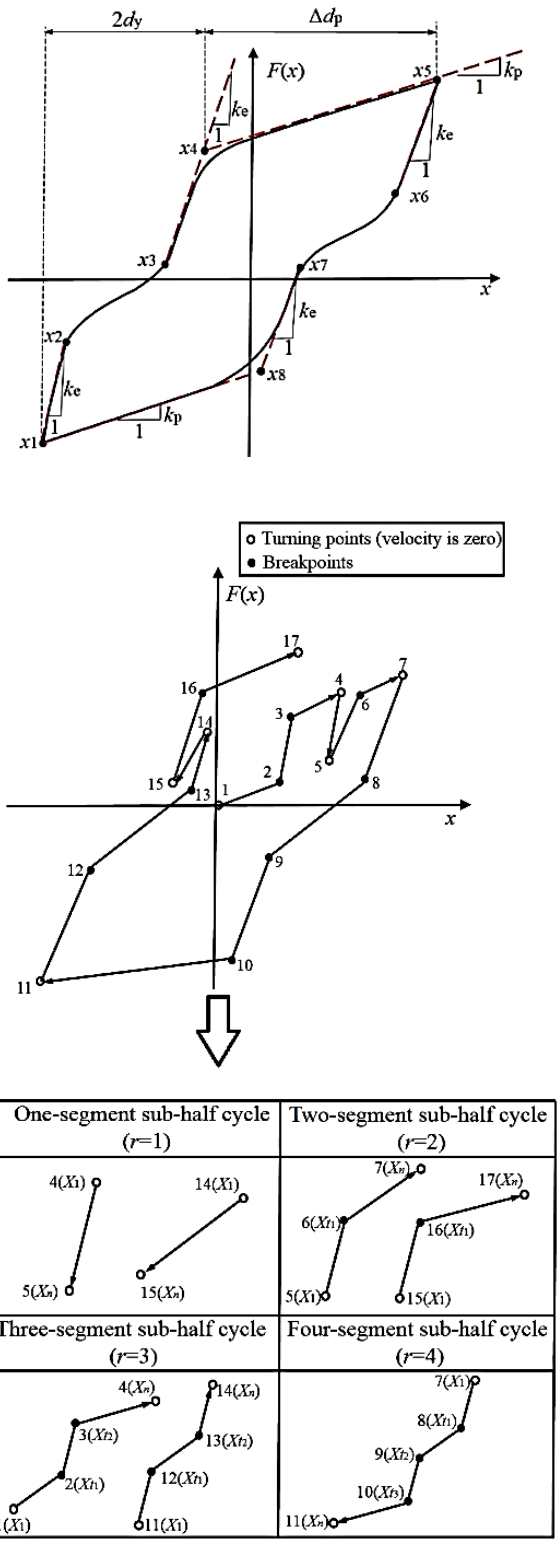

Figure 2: Examples of how HLA uses half-cycles and hysteresis loops to identify linear and nonlinear stiffness values. TOP Left) General nonlinear hysteresis loop for 2 half-cycles of response; TOP Right) A general example of 4 half-cycles of response; BOTTOM) the general example broken into individual half-cycles with differing numbers of segments up to r=4 segments.

While the details of the HLA method are presented elsewhere [40-43], the overall approach in this work undertakes the following steps:

- Segregate half-cycles of measured response for each (measured) storey.
- Create force-displacement hysteresis loops using storey acceleration and motion for each storey's inter-storey motion using the known or estimated story mass.
- Assess up to 4 stiffness values for each of up to 4 segments in each half-cycle using a statistical test [41] to find the optimal number of segments, where Figure 2 shows example cases to illustrate the method.
- Track the trajectory of linear stiffness values (and changes) over time to assess damage, where nonlinear motion and deflection are also tracked and provide further assessments of damage.

The outcome is thus the linear story stiffness trajectory over the entire ground motion event. Over multiple events, the final stiffness of one event is within 5% of the initial value of the subsequent event, as should be expected [43, 44].

This research hypothesizes the linear stiffness trajectory can be used as the input to a simplified structural model, which can be automatically created. If valid, the simulation in this model of the ground motion would yield the same, or very similar, displacement response metrics as the experimental test. This outcome would in turn validate the idea of using this model to rapidly evaluate immediate and longer-term safety and repair options – a critical first step beyond damage assessment.

Structural Model and Simulation

The structure is a 3-storey apartment building where each storey is instrumented. The equation of motion chosen for a simplified, readily automated model of this multi-degree-of-freedom inelastic structure subjected to earthquake excitation is defined:

$$Q\big(V(t)\big) = -MI\ddot{x}_g(t) - M\ddot{V}(t) - C(t)\dot{V}(t) \tag{1}$$

where $V(t), \dot{V}(t)$ and $\ddot{V}(t)$ are displacement, velocity and acceleration vectors, M is the constant mass matrix, and $C(t)$ is a Rayleigh damping matrix in this case. $Q\big(V(t)\big)$ is the nonlinear time-varying restoring force vector determined by the time-varying structural stiffness matrix $K(t)$ and loading-unloading path. In particular, the E-Defense test structure is a three-story SMRF building. Thus, M, $K(t)$, $C(t)$ and $Q(V(t))$ are easily defined:

$$M = \begin{bmatrix} m_1 & 0 & 0 \\ 0 & m_2 & 0 \\ 0 & 0 & m_3 \end{bmatrix} \tag{2}$$

$$C(t) = a_0 M + a_1 K(t) = \begin{bmatrix} C_{11}(t) & C_{12}(t) & 0 \\ C_{21}(t) & C_{22}(t) & C_{23}(t) \\ 0 & C_{32}(t) & C_{33}(t) \end{bmatrix} \tag{3}$$

$$K(t) = \begin{bmatrix} K_1(t) + K_2(t) & -K_2(t) & 0 \\ -K_2(t) & K_2(t) + K_3(t) & -K_3(t) \\ 0 & -K_3(t) & K_3(t) \end{bmatrix} \tag{4}$$

$$Q\big(V(t)\big) = \begin{bmatrix} Q_1(t) \\ Q_2(t) \\ Q_3(t) \end{bmatrix} = \begin{bmatrix} f_1(t) - f_2(t) \\ f_2(t) - f_3(t) \\ f_3(t) \end{bmatrix} \tag{5}$$

$$\begin{aligned} f_1(t) &= Q_1(t) + Q_2(t) + Q_3(t) \\ f_2(t) &= Q_2(t) + Q_3(t) \\ f_3(t) &= Q_3(t) \end{aligned} \tag{6}$$

where m_1, m_2 and m_3 are the mas for the first, second and third story, respectively. $K_1(t), K_2(t)$ and $K_3(t)$ are the time-varying story stiffness values identified using HLA. Parameters a_0 and a_1 are mass-proportional and stiffness-proportional damping coefficients based on Rayleigh damping model using *M* and *K(t)* [45], yielding time-varying damping, *C(t)*. To calculate a_0 and a_1, the damping ratio is assumed to

be 5% for the first and the highest third modes, respectively. Thus, the damping ratio for the second mode has a slight smaller value of 4.4% to satisfy the Rayleigh damping assumption.

It is noted that damping ratio in real structures are not necessary purely viscous, and change over time and earthquakes, thus making damping identification problematic. Thus, the Rayleigh damping model might not yield an accurate estimation of the true damping force, particularly for a nonlinear structure. However, the prior study has shown the damping force is a relatively small part of the total damping force in the elastic segments [44]. Therefore, assuming a damping ratio of 5% for Rayleigh model typically used in spectral design analyses to approximately add damping effect in the total restoring force can still yield a reasonable change of stiffness for damage indication and health monitoring [44, 45], although further study on the assessing the real coupled damping effect should be investigated with a more complex nonlinear model.

Finally, $f_1(t), f_2(t)$ and $f_3(t)$ are the net hysteretic restoring forces on each floor based on $f = K(t)*V(t)$, which thus define the elements of the vector, Q, or $Q_{1,2,3}(t)$ the nonlinear restoring forces for each storey. Figure 3 shows the simplified model, where it is clear such a modelling approach could be automated given identified $K(t)$ values, mass M, and measured displacements and accelerations.

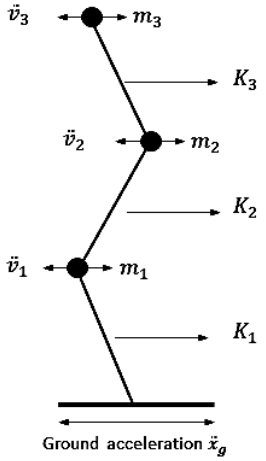

Figure 3: Simplified model structure and degrees of freedom used in both x and y directions, where the experimental structure did not have torsional response [44], which could be included as required.

Importantly, the model of Equations (1)-(5) is nonlinear with a time-varying stiffness and damping component varying with the identified stiffness changes, as seen specifically in Equations (3)-(4). Thus, the model structure is relatively quite simple, while containing potentially significant nonlinearity. Such a simple model is important, as initial decision-making will require an overall approach, and thus a detailed analysis may not be necessary or possible.

Equally importantly, the model structure itself cannot be any more "dense" than the measurement density. In this case, the structure was measured at a story level in multiple directions. Thus, a model at story level should be considered appropriate. Given there was little torsion observed, the actual analysis utilizes two such models, one for each of the x and y directions. Overall, the model used thus matches the sensor density in terms of relevant response degrees of freedom, and, in turn, dictates the complexity of the model created.

The next step is to turn identified trajectories of storey stiffness, $K(t)$, in both x and y directions into simplified functions of time for ready model simulation. Figures 4 and 5 show the identified storey stiffness trajectories over all six events in both x-direction and y-direction, respectively. Significant stiffness drops were identified for event 4 in both directions due to the much stronger input PGA of test #4 as listed in Table 1. In addition, the major stiffness change for event 4 occurs approximately between 12.5~15 seconds in Figures 4 and 5, corresponding to the strong shaking of the ground motion [44]. Stiffness trajectories were lightly smoothed using either a moving average or a wavelet filter [44]. While both versions are very similar, it is important to note the final stiffness values for each event are within 5% of the next event's initial identified stiffness value. This event-to-event consistency and accuracy is evident for each storey and event in both directions.

Linear functions are used to simply and algorithmically convert Figures 4 and 5 into readily simulated $K(t)$ functions for each storey, as a series of linear lines. Changes less than 5% are considered constant. It assumes stiffness changes occur over a finite time, where linear lines are simple, reasonable approximations, readily created automatically via simple algorithms from the HLA results in Figures 4 and 5. Figure 6 shows an example using 3 segments for the 1st story in x direction during Event 1. Table 2 shows the number of segments used in each story and event.

Table 2: Linear approximation of stiffness evolution for all 6 events and both (x,y) directions in Figures 4 and 5.

Event	x-direction			y-direction		
	1st story	2nd story	3rd story	1st story	2nd story	3rd story
#01	3	3	1	3	3	1
#02	3	3	3	3	3	1
#03	3	1	3	1	3	1
#04	4	4	4	4	4	4
#05	1	1	1	1	1	1
#06	4	4	4	4	4	4

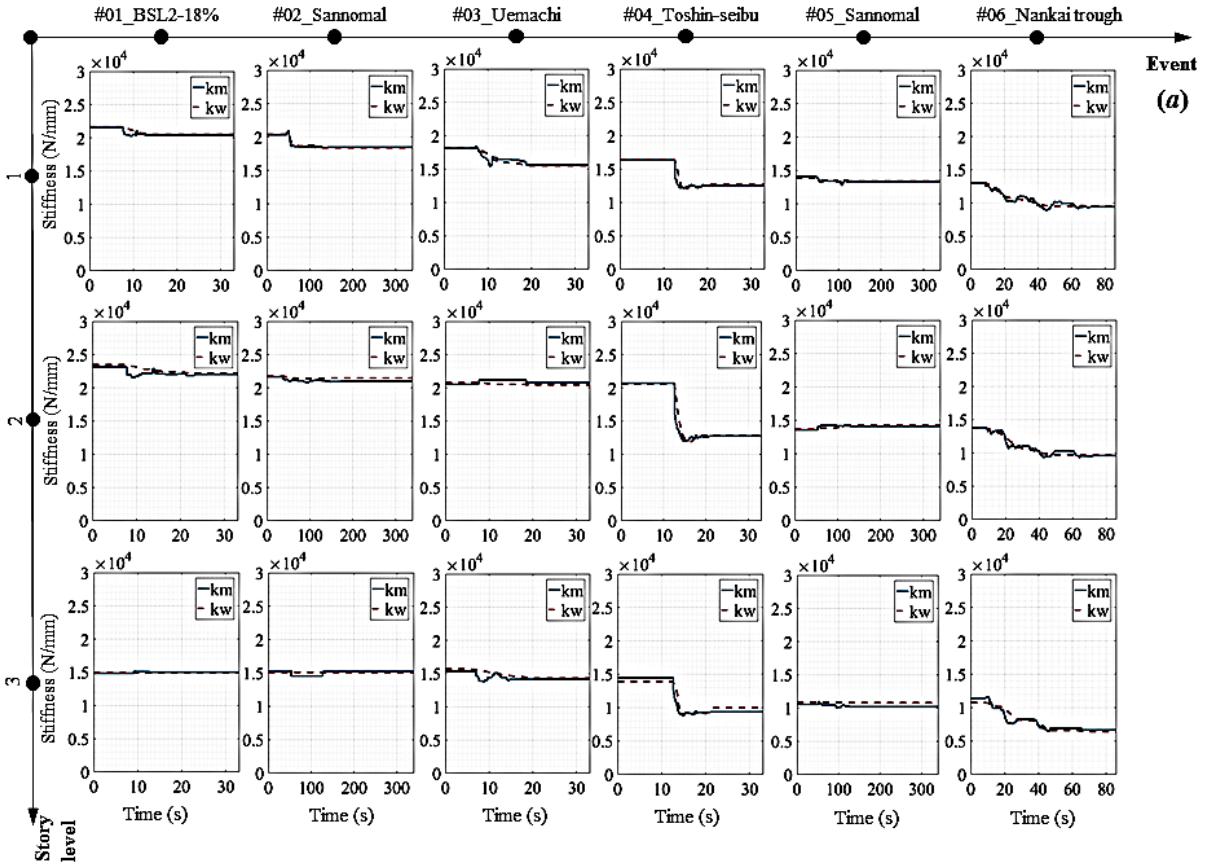

Figure 4: Identified evolution of effective elastic stiffness (ke) in the x-direction over events. The solid line km represents the moving average stiffness and the dashed line kw represents the wavelet stiffness, from [44].

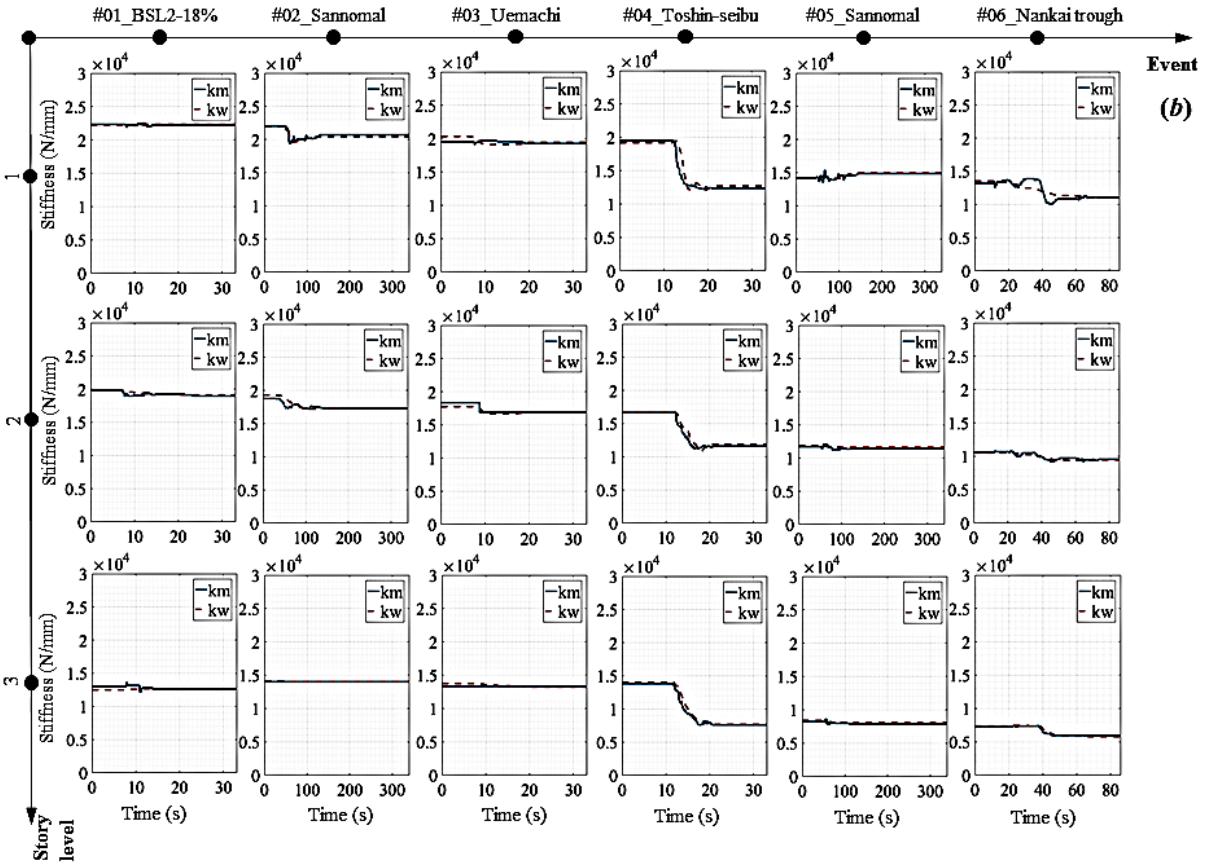

Figure 5: Identified evolution of effective elastic stiffness (ke) in the y-direction over events. The solid line km represents the moving average stiffness and the dashed line kw represents the wavelet stiffness, from [44].

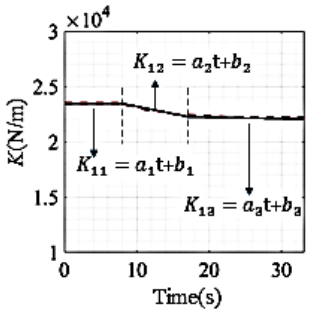

Figure 6: Example of linear approximation for the 1st story in x-direction during Event#1.

Analyses and Evaluation

Simulations use the Newmark-Beta method and a 0.005 seconds time step matching the experimental sampling rate. All six events are simulated using the model of Equations (1)-(6). Simulation responses are compared to measured time history responses, where differences would be due to the simple, readily automated model constructed and/or any error in the identified $K(t)$ profiles. The results thus assess both the accuracy of the simple model creation method presented and provide an overall validation of the stiffness values found by the HLA method:

Two metrics compare simulated and measured response for all events (6), stories (3), directions (x, y):

- **Peak Absolute Displacement Error**: A metric associated with structural damage.
- **Correlation Coefficient (R_{coeff})**: A metric capturing whether the two displacement responses compared have the same specific shape over time. It is more rigorous than the typically used average absolute error as it includes accuracy in point to point changes in the displacement responses over time. A value of 1.0 indicates a perfect match in magnitude at each point and a value of 0.0 the worst. Given differences in peak displacements, a value over 0.7-0.8 would be very good qualitatively when plotted.

These metrics assess the quality of the simple model, which can be automatically created, to match the structural response using the identified $K(t)$. As noted, a good match would validate the approach to generating models for further decision making from SHM results, as well as providing further validation of the HLA identified stiffness values.

Finally, a damping coefficient of 5% for the first and third modes was assumed using Rayleigh damping, leading to a time varying damping matrix based on how stiffness changed over time. The choice of 5% is arbitrary and commonly used [45]. However, a sensitivity analysis for different damping values is performed comparing correlation coefficients for each value to quantify its impact.

RESULTS AND DISCUSSION

Table 3 shows peak absolute errors for each event (#1-6), direction (x,y) and storey (1-3), where error estimating displacements from experimental accelerometer and other measurements is 0.5-1.0 mm depending on magnitude for the method used here [41, 46]. Figure 7 shows the 3rd storey x and y displacement responses, measured and simulated, for all 6 events during periods of strong motion. Finally, Table 4 shows the correlation coefficients for each event.

Table 3 has median [75th percentile] absolute errors of 0.84 [1.99] mm. The median is within estimation error, where 21 of 36 are less than 1.0 mm and the 75th percentile is relatively small. The 90th percentile error is 2.96 mm. Thus, the overall peak response is captured well, although not perfectly.

Table 3: Peak absolute displacement error (mm) between simulated and measured response for all 3 storey's and all 6 events in both x and y directions.

Event	x-direction			y-direction		
	1st story	2nd story	3rd story	1st story	2nd story	3rd story
#01	0.17(2.3%)	0.01(0.2%)	0.39(16.3%)	0.30(4.6%)	0.21(2.3%)	0.77(20.6%)
#02	0.84(12.3%)	0.46(8.9%)	0.67(23.0%)	0.70(8.5%)	0.15(2.1%)	0.19(4.0%)
#03	0.50(2.8%)	0.87(11.8%)	1.09(17.1%)	2.09(19.6%)	1.30(14.4%)	0.70(14.8%)
#04	2.96(6.6%)	3.96(12.0%)	2.32(11.6%)	6.27(14.1%)	2.34(5.9%)	4.49(15.6%)
#05	1.02(10.4%)	0.54(7.8%)	0.39(10.1%)	0.93(5.7%)	0.80(5.8%)	0.48(5.2%)
#06	2.58(4.7%)	2.96(6.9%)	3.82(14.8%)	1.19(3.1%)	1.99(6.0%)	0.43(1.9%)

Table 4: Correlation coefficients, R_{coeff}, for all events, storeys and directions, including mean value across all storeys and directions.

Event	x-direction			y-direction			x & y
	1st story	2nd story	3rd story	1st story	2nd story	3rd story	Mean
#01	0.89	0.86	0.85	0.93	0.91	0.87	0.89
#02	0.91	0.88	0.81	0.82	0.82	0.72	0.83
#03	0.82	0.77	0.77	0.62	0.60	0.72	0.72
#04	0.88	0.84	0.80	0.81	0.79	0.75	0.81
#05	0.89	0.86	0.79	0.86	0.86	0.79	0.84
#06	0.87	0.84	0.80	0.89	0.88	0.83	0.85

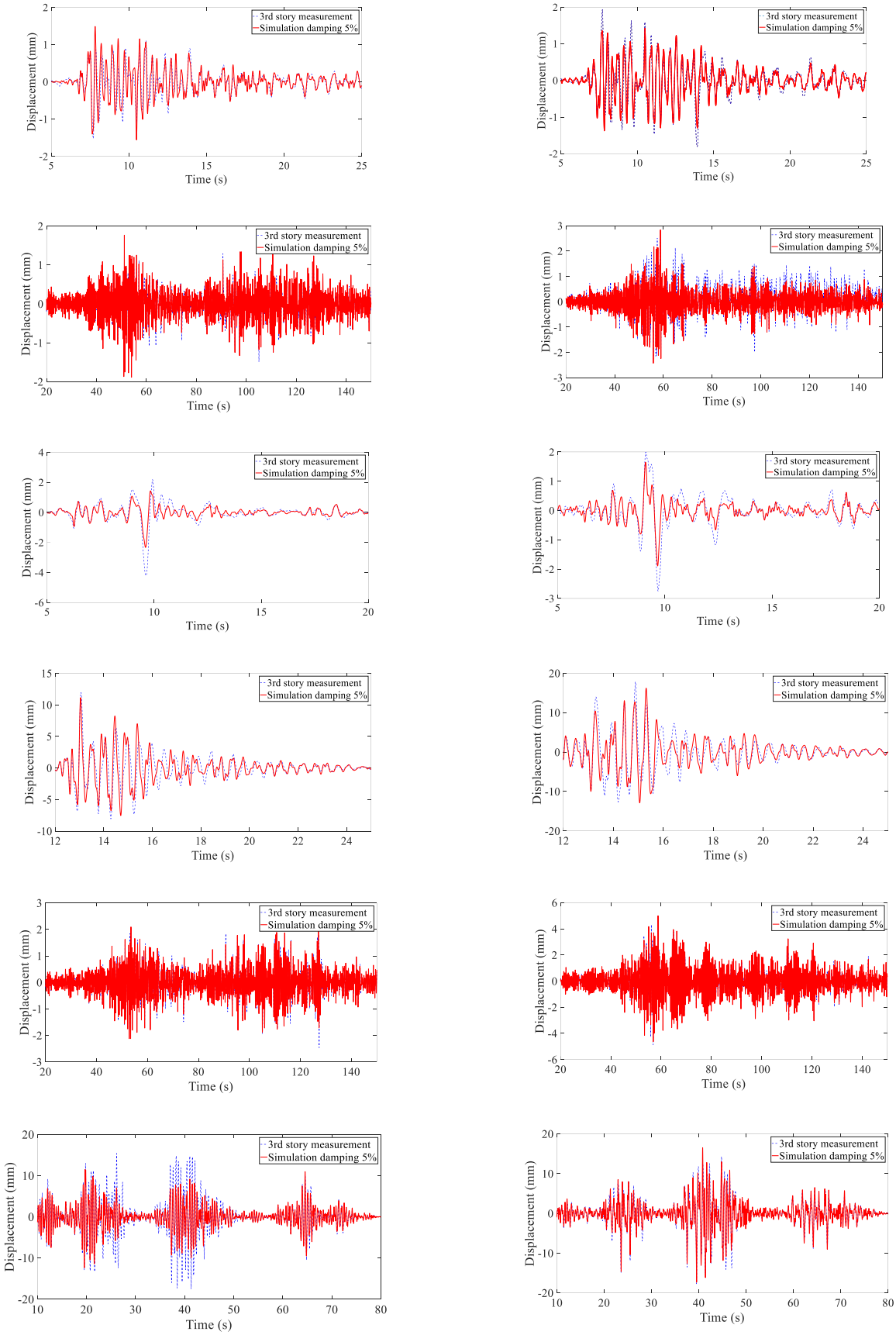

Figure 7: Third storey displacement over the long motion period for each of the 6 events (top to bottom) to show qualitative model comparison in both x (left) and y (right) directions, where blue dashed lines are the experimental measurements. The linear estimation of the model is used in this case. Note x and y axis scales are different between events.

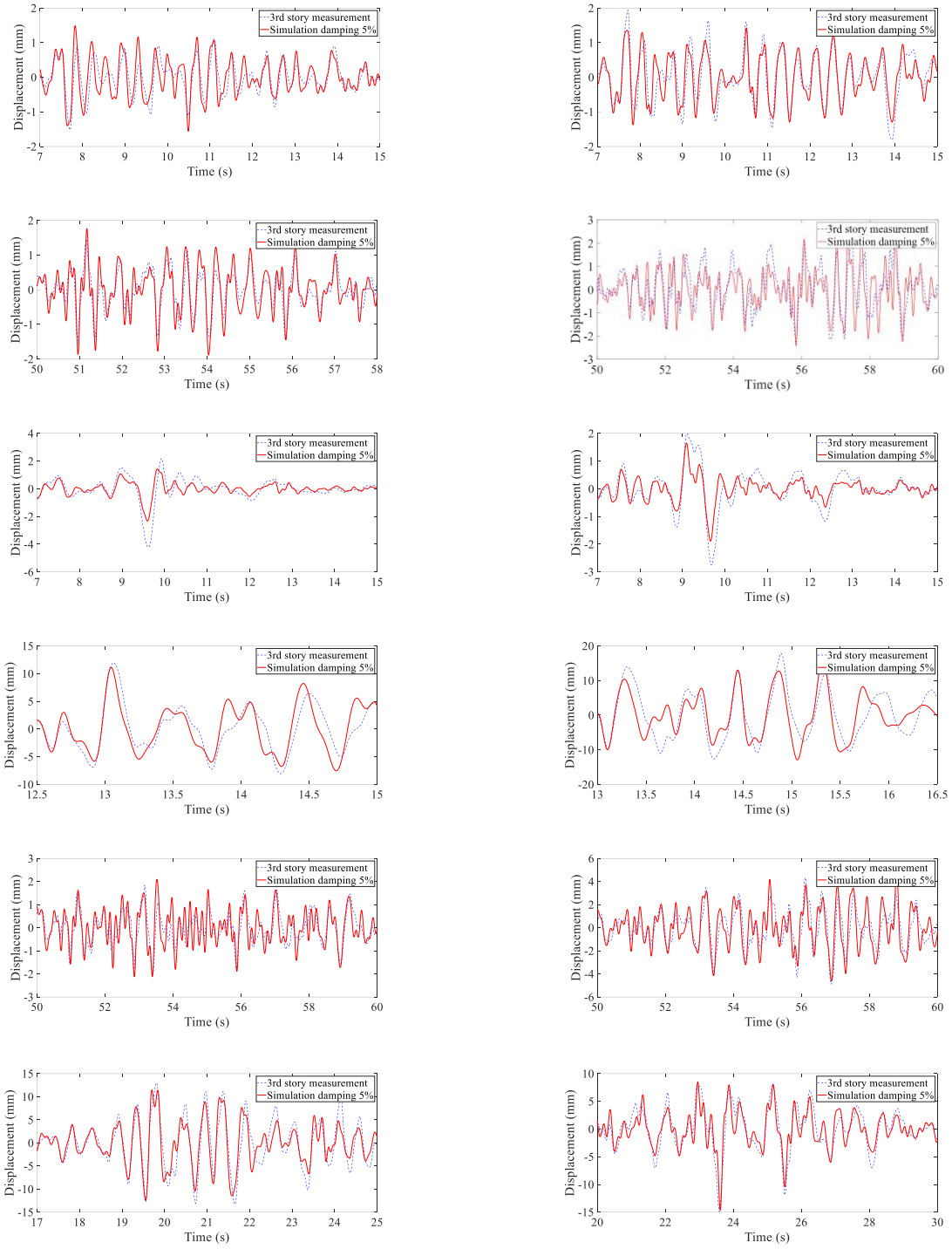

Figure 8: Third storey displacement over the strong motion for each of the 6 events (top to bottom) to show qualitative model comparison in both x (left) and y (right) directions, where blue dashed lines are the experimental measurements. The linear estimation of the model is used in this case. Note x and y axis scales are different between events.

In all cases, the modelled motion is a good match for the measured motion with correlation coefficients averaging 0.72-0.89 (0.82 overall) for all storeys, directions, and events. The third ground motion input is the worst with R_{coeff} = 0.71, and eliminating it raises the average to 0.85. Qualitatively, in Figure 7, the worst case for the third storey, and in general (results not shown), is the *x*-direction for Event #6 where there are clear underestimations of motion, which is reflected in the relatively lower R_{coeff} = 0.80 in Table 4 and larger 3.82mm differences seen in peak values in Table 3. It is still important to notice the record is long and much of it matches well, although not as visibly well for portions.

This relatively poorer result in the *x*-direction for Event #6 is offset by qualitatively very good results for the *y*-direction with slightly higher R_{coeff} = 0.83 in Table 4. This comparison shows there may be differences in the simplified model chosen and the actual structure, as should be expected. However, these differences are not enough to alter what are otherwise qualitatively good correlation results, where it is important to reiterate the correlation coefficient is a more rigorous test of accuracy than any single point or group of points comparison.

By further comparison, the correlation coefficients for Event #6 are much better than the worst case Event #3, despite what might appear in Figure 7 to be a better overall qualitative match

for Event #3. In this case, in Figure 7, Event #3 tracks very well despite not hitting some peak values as well. However, the point to point correlation of changes, the shape of the response, is not as good. This difference thus highlights not only model goodness, but also the impact of metrics chosen.

More specifically, using the correlation coefficient places value on the step-to-step shape of the response over time. It thus has lesser weight for peak values, which may also be important. Thus, this analysis uses Table 3 to provide a damage related metric of model fit and goodness. In turn, Table 4 and the correlation coefficient evaluates the model's overall quality in capturing dynamics. Together, they provide an overall view of the model's capability to represent the structure. More succinctly, all models and modelling approaches have advantages and limitations, and these different metrics used in this work provide a contrast across this range of ways to assess model function and capability.

Figure 9 shows the impact of the choice of damping ratio from 5-20% on the average correlation coefficient for each event. As with the prior results, Event #3 was the lowest overall followed by Event #4. Assuming a value of $R_{coeff} = 0.80$ as a minimum, excluding Event #3, then values of 8% and 10% offered slight improvements in correlation coefficient. These results first suggest the choice of 5% is conservatively low, but acceptable. Second, the choice of damping value plays a lesser role in how well this simplified modelling approach captures the resulting dynamics. Using a "best" value of 8% raised the overall average correlation coefficient to $R_{coeff} = 0.87$, which is not significantly higher than $R_{coeff} = 0.82$ ($R_{coeff} = 0.82$ without Event #3) found for the initial, typical 5% value chosen.

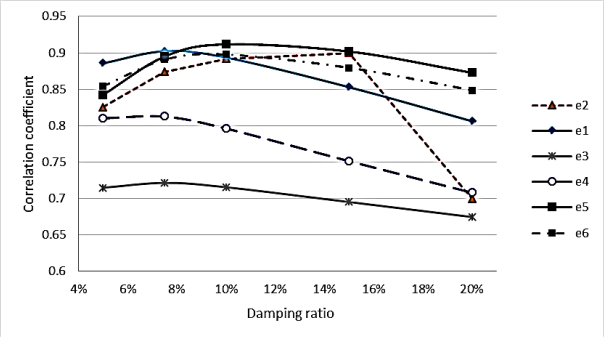

Figure 9: Average correlation coefficient for each event as a function of damping ratio chosen.

Combining all these results shows the simplified modelling approach provides a good and functional model on which further mitigation or other analyses could be based. The method is very simple to create and could thus be readily automated. Hence, the outcome SHM result using the HLA method is not only damage and localisation, but can also include reasonable baseline dynamic models for further analysis and assessment.

In terms of limitations it is important to note, while the specific method presented is simple enough to be automated, far more complex models could be readily generated. However, the ability to automate more complex model generation would be reduced. Thus, more complex modelling approaches could reduce the method's generalisability and likely require human input where automation could have the result ready in near real-time. Equally, the model density of degrees of freedom would likely exceed the measured density and would thus have to rely on assumptions of validity for motions in between those points, which could offer insight, but also risk in terms of model validity.

That all said, a more complex model than the simple shear structure of 3 degrees of freedom used here could possibly produce better results with minimal added effort. In this case, the model structure choice was made as simple as possible to demonstrate the potential of the approach. A more detailed analysis would be required to assess how simple or complex a model might be required for a given case, where this analysis shows the potential for a real structure.

However, and equally importantly, the relatively quite simple three degree of freedom models used here for each direction, captured the data very well, and thus a main outcome of the analysis is also how well such a relatively quite simple can perform when given the proper nonlinear inputs for stiffness changes. In this case, the model is almost absurdly simple, yet matches data very well. This outcome indicates the validity of the SHM method, as well as the need for little additional complexity in subsequent, initial model generation. In further analysis, one could of course add additional nonlinearities for better future prediction.

Equally, the linear damage approach is simple and provided good results. These results indicate the losses of lateral story stiffness for this 3-story E-Defense real building can be well identified and further used as damage indices in future health monitoring for a quick decision, considering the overall approach can be done within a few seconds with this simplified foundation model. However, a more accurate or complex realisation of the time-varying stiffness in Figure 4 might have resulted in a more accurate outcome, where errors in peak displacement in Table 3 might have been lower with a more accurate representation of the change in stiffness due to damage.

Again, there is a potential trade off and compromise amongst increasing complexity, increasing accuracy, and simplicity / automation [47]. A more complex model would yield a more accurate results, while it would require more *a-prior* knowledge of the structure and engineering analysis, take much longer time to process, and may also suffer the identifiably and model mismatch issues [15, 48]. In this case, the results were considered "good enough". However, the real assessment of accuracy is a function of the eventual outcome use intended, which was not the scope of this work.

The overall results show the potential and limitation of using a simplified model with HLA SHM results for automated modelling and dynamic analysis when applied to a real apartment building structure. The major limitation of the simple model is the lack of its ability to represent the exact nonlinear behaviour for detailed structural elements and/or complex modal response, but provides the estimates of the fundamental dynamics of the lateral vibration. Structures with a more complex nonlinear behaviours would require a more degrees of freedom and complex hysteretic model to represent the significant dynamics, which in turn requires a more complex and dense instruments. Therefore, a future work would be needed to investigate how complex a model should be choose with limited number of sensors.

Finally, regarding the relative importance of this work, here are many model-based SHM methods (e.g. [2-4, 6-13, 16-24]). In these cases, the model is at the heart of the SHM method and simulating the identified model will provide a response as good as the identification fit. However, and very importantly, if the model chosen is not a good match, the identification will be inaccurate [14, 15]. In this case, one has a good model in terms of replication, but the damage identification is inaccurate or misleading. This latter issue is critical as it means any use of the model to evaluate damage mitigation for safety or re-occupancy will be in error, potentially significantly so.

Because the HLA method is model-free, it requires some form of model creation approach to provide further value beyond damage localization and quantification. There are several

model-free approaches (e.g. [25-32, 34, 35]). Such an approach would potentially work with some of these SHM methods, as well. However, a similar approach could be used to assess the potential with other SHM methods. Hence, one main novelty and outcome of this work is the ability of the approach to generate an accurate valid model, which in turn can enable better decision-making post-event and serve as a baseline on which to build further models for more in-depth analysis and decisions.

There is thus a contradiction between the identification approach used for SHM and the possible end-uses. Equally, the limitations of the approach, such as model-based SHM error due to a mismatch in structural model and monitored structure behaviour, trade off with the same end uses. This work thus utilises the HLA method as it is model-free, avoiding these model-method mismatch issues, but also because of its proven accuracy and consistency across multiple events experimentally and as quantified analytically [40-44, 46, 49-51], where, to date, no other method has demonstrated both its accuracy and its consistency over multiple events.

These issues are little to not-at-all discussed in the SHM community. There is thus a strong and growing need to consider these alternatives and issues in developing effective SHM and extending its use, efficacy, and thus benefit.

CONCLUSIONS

This paper presents a simplified model creation method for use with model-free structural health monitoring methods. The goal is to create accurate baseline models using data from SHM damage identification and localisation methods to create models suitable for further investigation and analysis on safety, damage mitigation, and thus re-occupancy. Such models would take SHM from being a tool for damage identification and extend them into further decision-making, creating far greater utility for engineers and owners, which could further spur impetus for investment in monitoring.

The specific method presented is validated against experimental data from the E-Defense facility in Japan for a 3-storey apartment structure subjected to six events and suffering significant damage in some but not all events. Comparison of model results to the experimental data shows qualitatively good matches for peak displacements and correlation coefficients, where the first metric assesses damage and design related outcomes, and the second assesses how well the overall structure dynamics are captured. In general, results were very good and demonstrate a good baseline model can be generated for immediate use and longer-term evaluation of structural outcomes and mitigation.

A further main outcome is that a relatively simple model structure can yield a reasonable accuracy of the replicated response with nonlinearities in a given strong earthquake input for a real structure, validating the potential of this simple model generation to provide an near-real time dynamic analysis for decision making, as well as extending to a more complex model creation. However, the method still remains to be further validated for combined soil-structure system and/or other scenarios in a real application, in which more complex dynamics and higher mode response might be coupled in the vibration.

In terms of limitation, the effect of soil-structure interaction (SSI) is not considered in the dynamic modelling and analysis for the proposed algorithm. Such SSI might have significant effect on structure damping, period and thus response spectrum, particularly for very soft soil condition. These effects were quantified in a large series of Monte Carlo analyses by Moghaddasi et al quantifying the risk of exceedance in predicted response (or reduction) due to SSI effects with moderate and soft soils for linear and nonlinear structures [52-56]. This series of detailed analyses show the response compared to fixed base assumptions is similar or smaller at least 75-85% of the time, but for ~ 5-10% of cases, the risk of even larger displacements and response occurs due to SSI effects and soft soils. However, such simulation analysis does not necessary represent the true reality of SSI effect. Thus, the method still remains to be fully validated using real building data under different soil conditions. Equally, given the requirement of a ground motion measurement at the structural foundation, the “true input” to the structure, including modification due to SSI, is incorporated in both the HLA identification, as well as in the input for any future events. Overall, the robustness of the HLA method and this automated modelling approach for accurate prediction under soft soil conditions still remains to be completely validated before a pragmatic application in these types of sites.

The method is simple and generalizable. It can be readily extended to more complex models or other similar approaches using different modelling approaches depending on the sensor density and resolution of SHM results. Future work should also consider extending these methods to creating far more predictive, nonlinear models if possible, especially given the Christchurch series of earthquakes where major shocks were followed by almost equally large second shocks.

REFERENCES

1 Rafaa Abbas AH (2016). "Stability Analysis of the Seismic Response of High Rise Steel Buildings Including P-Delta Effects". *Applied Research Journal*, **2**(8): 353-361.

2 Chase J, Leo Hwang K, Barroso L and Mander J (2005). "A Simple Lms - Based Approach to the Structural Health Monitoring Benchmark Problem". *Earthquake Engineering and Structural Dynamics*, **34**(6): 575-594. https://doi.org/10.1002/eqe.433

3 Chase JG, Spieth HA, Blome CF and Mander J (2005). "Lms - Based Structural Health Monitoring of a Non - Linear Rocking Structure". *Earthquake Engineering and Structural Dynamics*, **34**(8): 909-930. https://doi.org/10.1002/eqe.460

4 Nayyerloo M, Chase J, MacRae G and Chen X (2011). "Lms-Based Approach to Structural Health Monitoring of Nonlinear Hysteretic Structures". *Structural Health Monitoring*, **10**(4): 429-444. https://doi.org/10.1177/1475921710379519

5 Chase JG, Begoc V and Barroso LR (2005). "Efficient Structural Health Monitoring for a Benchmark Structure Using Adaptive Rls Filters". *Computers and Structures*, **83**(8-9): 639-647. https://doi.org/10.1016/j.compstruc.2004.11.005

6 Huang H, Yang JN and Zhou L (2010). "Comparison of Various Structural Damage Tracking Techniques Based on Experimental Data". *Smart Structures and Systems*, **6**(9): 1057-1077. https://doi.org/10.12989/sss.2010.6.9.1057

7 Lei Y, Chen F and Zhou H (2015). "An Algorithm Based on Two - Step Kalman Filter for Intelligent Structural Damage Detection". *Structural Control and Health Monitoring*, **22**(4): 694-706. https://doi.org/10.1002/stc.1712

8 Pan S, Xiao D, Xing S, Law S, Du P and Li Y (2016). "A General Extended Kalman Filter for Simultaneous Estimation of System and Unknown Inputs". *Engineering Structures*, **109**: 85-98. https://doi.org/10.1016/j.engstruct.2015.11.014

9 Yang JN, Lin S, Huang H and Zhou L (2006). "An Adaptive Extended Kalman Filter for Structural Damage Identification". *Structural Control and Health Monitoring*, **13**(4): 849-867. https://doi.org/10.1002/stc.84

10 Al-Hussein A and Haldar A (2015). "Structural Health Assessment at a Local Level Using Minimum Information". *Engineering Structures*, **88**(1): 100-110. https://doi.org/10.1016/j.engstruct.2015.01.026

11 Wu M and Smyth A (2008). "Real-Time Parameter Estimation for Degrading and Pinching Hysteretic Models". *International Journal of Non-Linear Mechanics*, **43**(9): 822-833. https://doi.org/10.1016/j.ijnonlinmec.2008.05.010

12 Wu M and Smyth AW (2007). "Application of the Unscented Kalman Filter for Real - Time Nonlinear Structural System Identification". *Structural Control and Health Monitoring*, **14**(7): 971-990.

13 Xie Z and Feng J (2012). "Real-Time Nonlinear Structural System Identification Via Iterated Unscented Kalman Filter". *Mechanical Systems and Signal Processing*, **28**: 309-322. https://doi.org/10.1016/j.ymssp.2011.02.005

14 Yao R and Pakzad SN (2014). "Time and Frequency Domain Regression - Based Stiffness Estimation and Damage Identification". *Structural Control and Health Monitoring*, **21**(3): 356-380.

15 Zhou C, Chase JG, Rodgers GW and Xu C (2017). "Comparing Model-Based Adaptive Lms Filters and a Model-Free Hysteresis Loop Analysis Method for Structural Health Monitoring". *Mechanical System and Signal Processing*, **84**(2017): 384-398. https://doi.org/10.1016/j.ymssp.2016.07.030

16 Juang J-N and Pappa RS (1985). "An Eigensystem Realization Algorithm for Modal Parameter Identification and Model Reduction". *Journal of Guidance, Control, and Dynamics*, **8**(5): 620-627.

17 Bernal D and Gunes B (2000). "Observer/Kalman and Subspace Identification of the Ubc Benchmark Structural Model". *Proceedings of the 14th ASCE Engineering Mechanics Conference*, Texas, 21-24.

18 Lus H, Betti R, Yu J and De Angelis M (2003). "Investigation of a System Identification Methodology in the Context of the Asce Benchmark Problem". *Journal of Engineering Mechanics*, **130**(1): 71-84.

19 Giraldo D, Yoshida O, Dyke SJ and Giacosa L (2004). "Control - Oriented System Identification Using Era". *Structural Control and Health Monitoring*, **11**(4): 311-326.

20 Dyke SJ, Caicedo JM and Johnson EA (2000). "Monitoring of a Benchmark Structure for Damage Identification". *Proceedings of the Engineering Mechanics Speciality Conference*, Austin, Texas, 21-24 May, 2000.

21 Bernal D and Levy A (2001). "Damage Localization in Plates Using Dlvs". *Proceedings of the 19th International Modal Analysis Conference*, 1205-11.

22 Bernal D (2002). "Load Vectors for Damage Localization". *Journal of Engineering Mechanics*, **128**(1): 7-14. https://doi.org/10.1061/(Asce)0733-9399(2002)128:1(7)

23 Moaveni B, Conte JP and Hemez FM (2009). "Uncertainty and Sensitivity Analysis of Damage Identification Results Obtained Using Finite Element Model Updating". *Computer - Aided Civil and Infrastructure Engineering*, **24**(5): 320-334. https://doi.org/10.1111/j.1467-8667.2008.00589.x

24 García - Palencia AJ and Santini - Bell E (2013). "A Two - Step Model Updating Algorithm for Parameter Identification of Linear Elastic Damped Structures". *Computer - Aided Civil and Infrastructure Engineering*, **28**(7): 509-521.

25 Lozano - Galant JA, Nogal M, Castillo E and Turmo J (2013). "Application of Observability Techniques to Structural System Identification". *Computer - Aided Civil and Infrastructure Engineering*, **28**(6): 434-450. https://doi.org/10.1111/mice.12004

26 Jiang X and Adeli H (2005). "Dynamic Wavelet Neural Network for Nonlinear Identification of Highrise Buildings". *Computer - Aided Civil and Infrastructure Engineering*, **20**(5): 316-330. https://doi.org/10.1111/j.1467-8667.2005.00399.x

27 Adeli H and Jiang X (2006). "Dynamic Fuzzy Wavelet Neural Network Model for Structural System Identification". *Journal of Structural Engineering*, **132**(1): 102-111. https://doi.org/10.1061/(Asce)0733-9445(2006)132:1(102)

28 Graf W, Freitag S, Sickert JU and Kaliske M (2012). "Structural Analysis with Fuzzy Data and Neural Network Based Material Description". *Computer - Aided Civil and Infrastructure Engineering*, **27**(9): 640-654. https://doi.org/10.1111/j.1467-8667.2012.00779.x

29 Jiang X and Adeli H (2007). "Pseudospectra, Music, and Dynamic Wavelet Neural Network for Damage Detection of Highrise Buildings". *International Journal for Numerical Methods in Engineering*, **71**(5): 606-629. https://doi.org/10.1002/nme.1964

30 Arangio S and Bontempi F (2010). "Soft Computing Based Multilevel Strategy for Bridge Integrity Monitoring". *Computer - Aided Civil and Infrastructure Engineering*, **25**(5): 348-362. https://doi.org/10.1111/j.1467-8667.2009.00644.x

31 Osornio - Rios RA, Amezquita - Sanchez JP, Romero - Troncoso RJ and Garcia - Perez A (2012). "Music - Ann Analysis for Locating Structural Damages in a Truss - Type Structure by Means of Vibrations". *Computer - Aided Civil and Infrastructure Engineering*, **27**(9): 687-698.

32 Story BA and Fry GT (2014). "A Structural Impairment Detection System Using Competitive Arrays of Artificial Neural Networks". *Computer - Aided Civil and Infrastructure Engineering*, **29**(3): 180-190. https://doi.org/10.1111/mice.12040

33 Sirca G and Adeli H (2012). "System Identification in Structural Engineering". *Scientia Iranica*, **19**(6): 1355-1364. https://doi.org/10.1016/j.scient.2012.09.002

34 Adeli H and Jiang X (2009). "*Intelligent Infrastructure: Neural Networks, Wavelets, and Chaos Theory for Intelligent Transportation Systems and Smart Structures*". CRC Press, Taylor & Francis, Boca Raton, Florida.

35 Xiang J and Liang M (2012). "Wavelet - Based Detection of Beam Cracks Using Modal Shape and Frequency Measurements". *Computer - Aided Civil and Infrastructure Engineering*, **27**(6): 439-454.

36 Jiang X and Adeli H (2008). "Neuro - Genetic Algorithm for Non - Linear Active Control of Structures". *International Journal for Numerical Methods in Engineering*, **75**(7): 770-786.

37 Fuggini C, Chatzi E and Zangani D (2013). "Combining Genetic Algorithms with a Meso - Scale Approach for System Identification of a Smart Polymeric Textile". *Computer - Aided Civil and Infrastructure Engineering*, **28**(3): 227-245.

38 Yick J, Mukherjee B and Ghosal D (2008). "Wireless Sensor Network Survey". *Computer Networks*, **52**(12): 2292-2330. https://doi.org/10.1016/j.comnet.2008.04.002

39 Hu X, Wang B and Ji H (2013). "A Wireless Sensor Network - Based Structural Health Monitoring System for

Highway Bridges". *Computer - Aided Civil and Infrastructure Engineering*, **28**(3): 193-209.

40 Xu C, Chase JG and Rodgers GW (2014). "Physical Parameter Identification of Nonlinear Base-Isolated Buildings Using Seismic Response Data". *Computers and Structures*, **145**(1): 47-57. https://doi.org/10.1016/j.compstruc.2014.08.006

41 Zhou C, Chase JG, Rodgers GW, Tomlinson H and Xu C (2015). "Physical Parameter Identification of Structural Systems with Hysteretic Pinching". *Computer - Aided Civil and Infrastructure Engineering*, **30**(4): 247-262. https://doi.org/10.1111/mice.12108

42 Zhou C, Chase JG, Rodgers GW, Xu C and Tomlinson H (2015). "Overall Damage Identification of Flag-Shaped Hysteresis Systems under Seismic Excitation". *Smart Structures and Systems*, **16**(1): 163-181. https://doi.org/10.12989/sss.2015.16.1.163

43 Zhou C, Chase JG and Rodgers GW (2017). "Efficient Hysteresis Loop Analysis-Based Damage Identification of a Reinforced Concrete Frame Structure over Multiple Events". *Journal of Civil Structural Health Monitoring*, **7**: 541-556. https://doi.org/10.1007/s13349-017-0241-8

44 Zhou C, Chase JG, Rodgers GW and Iihoshi C (2017). "Damage Assessment by Stiffness Identification for a Full-Scale Three-Story Steel Moment Resisting Frame Building Subjected to a Sequence of Earthquake Excitations". *Bulletin of Earthquake Engineering*, **15**: 5393–5412. https://doi.org/10.1007/s10518-017-0190-y

45 Chopra AK (1995). "*Dynamics of Structures: Theory and Applications to Earthquake Engineering*". Prentice Hall, New Jersey, 794 pp.

46 Xu C, Chase JG and Rodgers GW (2015). "Nonlinear Regression Based Health Monitoring of Hysteretic Structures under Seismic Excitation". *Shock and Vibration*. https://doi.org/10.1155/2015/193136

47 Chase JG, Preiser J-C, Dickson JL, Pironet A, Chiew YS, Pretty CG, Shaw GM, Benyo B, Moeller K and Safaei S (2018). "Next-Generation, Personalised, Model-Based Critical Care Medicine: A State-of-the Art Review of in Silico Virtual Patient Models, Methods, and Cohorts, and How to Validation Them". *Biomedical Engineering Online*, **17**(1): 24. https://doi.org/10.1186/s12938-018-0455-y

48 Docherty PD, Chase JG, Lotz TF and Desaive T (2011). "A Graphical Method for Practical and Informative Identifiability Analyses of Physiological Models: A Case Study of Insulin Kinetics and Sensitivity". *Biomedical Engineering Online*, **10**(1): 39. https://doi.org/10.1186/1475-925X-10-39

49 Kuang A, Sridhar A, Garven J, Gutschmidt S, Rodgers GW, Chase JG, Gavin HP, Nigbor RL and MacRae GA (2016). "Christchurch Women's Hospital: Performance Analysis of the Base-Isolation System During the Series of Canterbury Earthquakes 2011-2012". *Journal of Performance of Constructed Facilities*, **30**(4). https://doi.org/10.1061/(Asce)Cf.1943-5509.0000846

50 Sridhar A, Kuang A, Garven J, Gutschmidt S, Chase JG, Gavin HP, Nigbor RL, Rodgers GW and MacRae GA (2014). "Christchurch Women's Hospital: Analysis of Measured Earthquake Data During the 2011-2012 Christchurch Earthquakes". *Earthquake Spectra*, **30**(1): 383-400. https://doi.org/10.1193/021513eqs027m

51 Zhou C, Chase JG, Rodgers GW, Kuang A, Gutschmidt S and Xu C (2015). "Performance Evaluation of Cwh Base Isolated Building During Two Major Earthquakes in Christchurch". *Bulletin of the New Zealand Society for Earthquake Engineering*, **48**(4): 264-273. https://doi.org/10.5459/bnzsee.48.4.264-273

52 Moghaddasi M, Chase J, Cubrinovski M, Pampanin S and Carr A (2012). "Sensitivity Analysis for Soil-Structure Interaction Phenomenon Using Stochastic Approach". *Journal of Earthquake Engineering*, **16**(7): 1055-1075.

53 Moghaddasi M, Cubrinovski M, Chase J, Pampanin S and Carr A (2011). "Effects of Soil–Foundation–Structure Interaction on Seismic Structural Response Via Robust Monte Carlo Simulation". *Engineering Structures*, **33**(4): 1338-1347.

54 Moghaddasi M, Cubrinovski M, Chase J, Pampanin S and Carr A (2012). "Stochastic Quantification of Soil-Shallow Foundation-Structure Interaction". *Journal of Earthquake Engineering*, **16**(6): 820-850. https://doi.org/10.1080/13632469.2012.661122

55 Moghaddasi M, Cubrinovski M, Chase JG, Pampanin S and Carr A (2011). "Probabilistic Evaluation of Soil–Foundation–Structure Interaction Effects on Seismic Structural Response". *Earthquake Engineering and Structural Dynamics*, **40**(2): 135-154.

56 Moghaddasi M, MacRae GA, Chase J, Cubrinovski M and Pampanin S (2015). "Seismic Design of Yielding Structures on Flexible Foundations". *Earthquake Engineering and Structural Dynamics*, **44**(11): 1805-1821. https://doi.org/10.1002/eqe.2556

APPENDIX A. HLA EXAMPLE

A single degree of freedom system was excited using *f*(*t*), as shown in Figure A-1. The parameters for the system are set in Table A-1. Figure A-2 shows the hysteresis loop of the simulated system under 1.5 cycles excitation *f*(*t*). Here we added 10% RMS noise to the simulated data.

Then we start to identify the pre-yielding stiffness (ke), the post-yielding stiffness (kp) and cumulative plastic deformation (Δdp) using the proposed method step by step, as shown in Figure A-3.

Table A-1: Set of parameters.

Mass	Post-yielding stiffness	Pre-yielding stiffness	Yield displacement	Damping ratio
1	1	0.1	1	5%

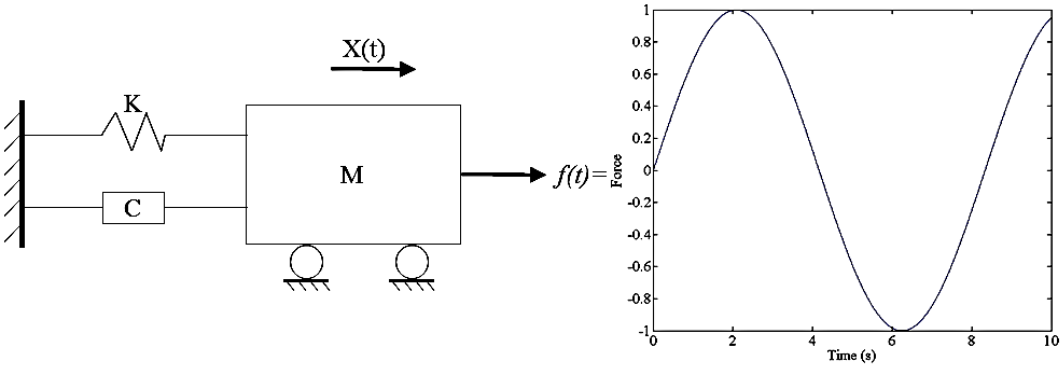

Figure A-1: Simulated system.

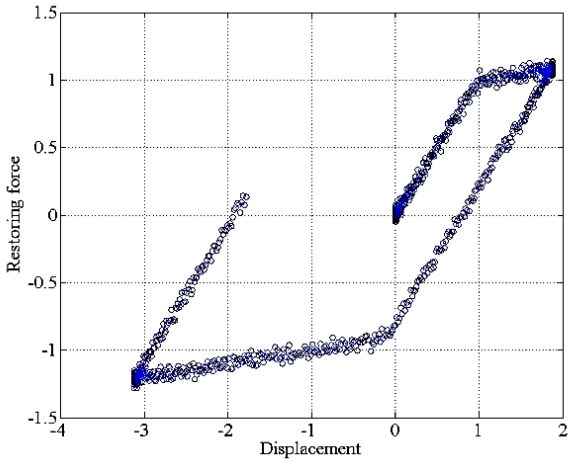

Figure A-2: Hysteresis loop of the simulated system.

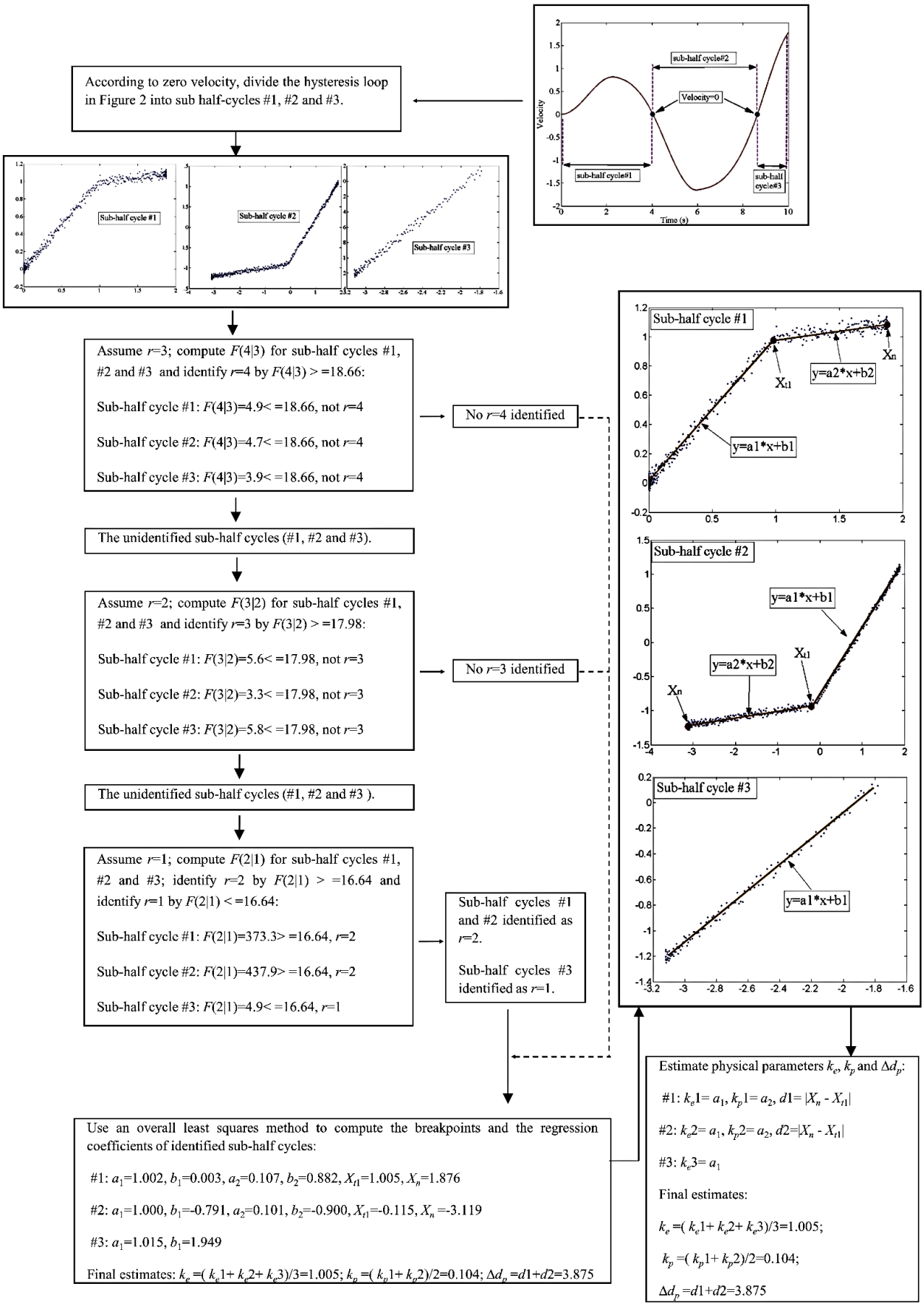

Figure A-3: Flowchart of HLA Implementation.